Quantum states of a hydrogen atom adsorbed on Cu(100) and (110) surfaces

Nobuki Ozawa,[1] Tanglaw Roman,[1] Hiroshi Nakanishi,[1] Wilson Agerico Diño,[2,3] and Hideaki Kasai[1,*]
[1]*Department of Precision Science & Technology and Applied Physics, Osaka University, Suita, Osaka, 565-0871, Japan*
[2]*Center for the Promotion of Research on Nanoscience and Nanotechnology, Osaka University, Toyonaka, Osaka 560-8531, Japan*
[3]*Department of Physics, Osaka University, Toyonaka, Osaka 560-0043, Japan*
(Received 31 March 2006; revised manuscript received 3 December 2006; published 26 March 2007)

Quantum states of a hydrogen atom adsorbed on Cu(100) and Cu(110) are studied theoretically. In calculating eigenenergies and wave functions of hydrogen atom motion, three-dimensional adiabatic potential energy surfaces (PESs) are constructed within density functional theory and the Schrödinger equation for hydrogen atom motion on the PESs is solved by the variation method. The wave function on Cu(100) indicates a localized mode on the hollow (HL) site at the ground state. Wave functions of the first few excited states indicate vibrational modes on the HL site and suggest migration from an HL site to a neighboring HL site over the bridge (BR) site. In the case of Cu(110), the ground state wave function is spread from the short bridge (SB) site and to the pseudothreefold (PT) site. The first few excited states are vibrational modes centered at the SB and long bridge (LB) sites. The excited state wave function of the hydrogen atom motion on Cu(110) show isotope effects as follows. The fourth excited state wave function for the H atom motion shows a localized character on the LB site, and those for D and T atom motion show vibrational modes parallel to the surface. On the other hand, the fifth excited state wave functions for D and T atom motion show localized characters on the LB site and that for H atom motion shows a vibrational mode parallel to the surface. Our calculated eigenenergies of the hydrogen atom motion in excited states on Cu(100) and Cu(110) are fairly in agreement with their corresponding experimental findings.

DOI: 10.1103/PhysRevB.75.115421 PACS number(s): 68.35.Ja, 68.43.Mn, 71.15.Mb, 82.20.Kh

I. INTRODUCTION

The study of how hydrogen behaves on solid surfaces is very useful in order to understand the dynamics of various reactions, and plays an important role in designing various industrial processes such as catalysis, hydrogen storage, and production of clean fuel. Spanning decades of research, a large number of studies have been carried out in order to obtain a clear understanding of the behavior of hydrogen on solid surfaces.[1] In line with this, it has been shown in recent years from both sides of experiment and theory that due to the small mass of hydrogen, it shows quantum effects, such as energy dispersion, tunneling, and delocalization on a solid surface.[2–9]

The behavior of hydrogen on the Cu surface has been studied through several different approaches—in experimental studies for example, by high resolution electron energy loss spectroscopy (HREELS),[10–12] low energy electron diffraction,[10,13] and scanning tunneling microscope (STM) based inelastic electron tunneling spectroscopy (IETS)[14] and in theoretical studies, by density functional theory (DFT) based first principles calculations for electronic states[3–9,15–18] and quantum dynamics simulations for dissociative adsorption of hydrogen molecules, hydrogen diffusion, absorption and associative desorption.[3,4,19–23] The behavior of a hydrogen atom on Cu(100) has been investigated theoretically by Lai *et al.*,[8] Sundell *et al.*,[9] and Kua *et al.*,[15] and on Cu(110) by Bae *et al.*[16] Save for the latter, these studies have treated hydrogen atom motion from a quantum mechanical perspective.

In this study, we pursue further details on the quantum mechanical behavior of adsorbed hydrogen (H, D, and T) on Cu(100) and (110). At first we construct the adiabatic potential energy surfaces (PESs) for hydrogen atom motion on Cu(100) and Cu(110) through first principles calculations based on density functional theory. We then solve the three-dimensional Schrödinger equation for hydrogen atom motion on the PESs by the variation method and obtain the corresponding wave functions and eigenenergies. From these results, we discuss the preferred adsorption states, vibrational states, the diffusion paths on the Cu(100) and (110) surfaces and the corresponding isotope effects by comparing the different quantum states for the hydrogen atom on the two Cu surfaces. Lastly, we compare our results with available experimental data.

The paper is organized as follows. Section II discusses briefly (1) the total energy calculations, (2) the construction of the adiabatic PES, and (3) the calculation of the corresponding wave functions and eigenenergies for hydrogen atom motion by the variation method. The calculation results, and discussions of the characters of the quantum states and the corresponding quantum effects in H, D, and T atom motion on Cu(100) and (110) follow in Sec. III. In the final section, we sum up the main points of this paper.

II. THEORY

A. Total energy calculations

Potential energy surfaces (PESs) for hydrogen atom motion on Cu(100) and Cu(110) were first constructed from density functional theory-based total energy calculations as a function of the position of the hydrogen atom on the surface. Our PES calculations were carried out through the first principles calculation code DACAPO,[25] which is a total energy calculation program based on DFT in a supercell geometry.

TABLE I. Calculated energies for hydrogen at high-symmetry sites on Cu(100) and Cu(110), with respect to the number of atomic layers. All values are expressed in eV.

Slab of Cu(100)	4 layer	6 layer	8 layer
Hollow	−2.485	−2.529	−2.464
Brige	−2.317	−2.401	−2.381
Top	−1.802	−1.748	−1.75
slab of Cu(110)	4 layer	6 layer	8 layer
Hollow	−2.065	−2.038	−2.108
long brige	−2.269	−2.314	−2.324
short brige	−2.353	−2.434	−2.387
pseudo three fold	−2.331	−2.411	−2.359
Top	−1.835	−1.765	−1.858

In our calculation, we use the generalized gradient approximation (GGA) to deal with the exchange correlation energies.[26] Ionic cores are described by ultrasoft pseudopotentials and we use a cutoff energy of 26 Ry to limit the plane-wave basis set. We sampled the surface Brillouin zone with a Monkhorst-Pack grid of $4\times4\times1$ k points. We used periodically repeated slabs of four atomic layers with a (2×2) unit cell, i.e., with a 0.25 monolayer (ML) hydrogen coverage. In these calculations, the lattice constant for Cu is fixed to 3.64 Å, the same value calculated for bulk Cu (experimental value:[27] 3.61 Å). Adjacent slabs are separated by a vacuum region of a size equivalent to six atomic layers, and all atoms of the slab are fixed because of negligible differences found with total energies from a slab composed of fully-relaxed substrate atoms with hydrogen on the surface. The negligible difference in the total energies is also implied in Ref. 8. We finally note that the energy origin of the PES is taken as the sum of the total energy of the isolated slab and that of an isolated hydrogen atom.

In order to see the influence of slab thickness, total energy calculations with the hydrogen atom positioned at high-symmetry sites were performed with four, six, and eight atomic layers representing the Cu(100) and Cu(110) surfaces. Table I shows the obtained results. The potential energy convergence with increasing the atomic layers shows that a four-layer slab is a reasonable approximation for constructing the PES used for determining wave functions and eigenenergies of H atom motion.

B. Construction of adiabatic PESs

The potential energy calculations were performed at $8\times8\times9$ $[8\times12\times9]$ grid points within the unit cell $[8\times8$ $[8\times12]$ grid points located in planes parallel to the Cu(100) [Cu(110)] surface, with nine planes]. To construct the adiabatic PESs for the hydrogen atom motion as shown in Fig. 1 and Table II, the PESs are represented by Morse-type potential energy curves along the surface normal direction, and hence take the following form:

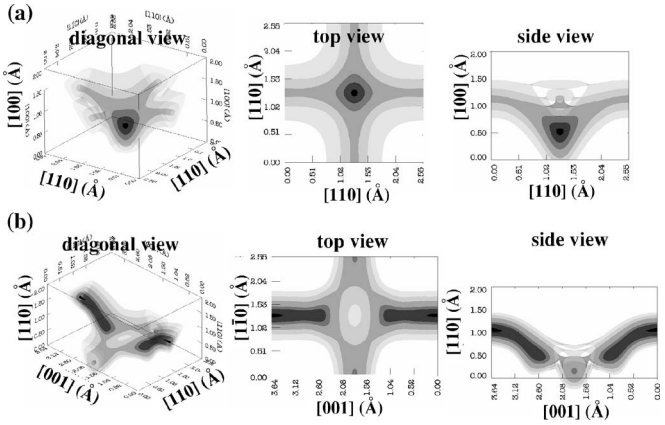

FIG. 1. Representations of the three dimensional potential energy surface for adiabatic hydrogen atom motion on Cu(100), from a diagonal view, top view (along the [100] axis) and side view (along the [01$\bar{1}$] axis). In increasing shading depth, the PES is represented by isosurfaces with values of −2.0, −2.20, −2.30, −2.40, −2.45, and −2.48 eV. Cu atoms are located at (0.00,0.00,0.00), (2.55,0.00,0.00), (0.00,2.55,0.00), and (2.55,2.55,0.00). (b) Same as (a), but for the top view (along the [011] axis) and side view (along the [01$\bar{1}$] axis) on Cu(110). In increasing shading depth, the PES is represented by isosurfaces with values of −2.0, −2.10, −2.16, −2.26, −2.30, and −2.34 eV. Cu atoms are located at (0.00,0.00,0.00), (3.64,0.00,0.00), (0.00,2.55,0.00), and (3.64,2.55,0.00).

$$U(x,y,z) = D(x,y)(\exp\{-\alpha(x,y)[z - z_0(x,y)]^2 - 1\}^2 - 1), \tag{1}$$

where z is the coordinate of the hydrogen atom perpendicular to the surface, and x and y are the coordinates parallel to the surface. $D(x,y)$, $z_0(x,y)$, and $\alpha(x,y)$ are the depth, the bottom position and the width of the Morse-type potential, respectively. These parameters are determined when the Morse-type potential energy curves fit the calculated potential energy values at the nine grid points in the direction perpendicular to the surface. In addition, the parameters are interpolated in the direction parallel to the surface by Fourier expansions in order to obtain smooth PESs.

C. Wave functions and eigenenergies

In order to investigate quantum states of the hydrogen (H, D, and T) atom motion, the three-dimensional Schrödinger equation for the hydrogen atom motion is solved on the constructed PESs with the aid of the variation method, taking into account periodic boundary conditions along the surface plane. The wave function of hydrogen atom motion is represented by a linear combination of Gaussian-type functions expressed explicitly as

$$\phi_i(x,y,z) = \left(\frac{\beta_x\beta_y\beta_z}{\pi^3}\right)^{1/4} \exp\left\{-\frac{1}{2}[\beta_x(x - X_i)^2 + \beta_y(y - Y_i)^2 + \beta_z(z - Z_i)^2]\right\}, \tag{2}$$

TABLE II. Calculated eigenenergies for hydrogen (H, D, and T) atom motion on the Cu(100) and Cu(100) surfaces. The origin of eigenenergy values is the ground state eigenenergy −2.339 eV (H), −2.383 eV (D), and −2.400 eV (T) on Cu(100) and −2.179 eV (H), −2.222 eV (D), and −2.240 eV (T) on Cu(110) (Ref. 24).

Cu(100) excited state	Protium Energy (meV)	Deuterium Energy (meV)	Tritium Energy (meV)
0	0	0	0
1	90.8	67.2	55.0
2	119	114	112
3	119	114	112
4	142	125	113
5	154	127	122

Cu(110) excited state	Protium Energy (meV)	Deuterium Energy (meV)	Tritium Energy (meV)
0	0	0	0
1	9.42	8.80	8.76
2	16.8	12.0	11.1
3	37.2	22.1	16.8
4	56.4	35.6	25.5
5	64.7	59.0	60.1
6	108	87.8	76.5
7	108	88.3	77.1
8	110	107	91.8
9	134	114	104
10	145	116	106

where the index i labels the Gaussian-type function whose center is at the grid point (X_i, Y_i, Z_i). The parameters β_x, β_y, β_z are adjusted so that the neighboring Gaussian-type functions overlap at half-maximum values. The Gaussian-type functions are placed at points on 6×6 [8×6] grids located on planes parallel to the Cu(100) [Cu(110)] surface, with planes separated by 0.2 Å and spanning the range $z=0.0$ to 1.8 Å. The wave functions and the corresponding eigenenergies for the hydrogen atom motion are obtained by solving the obtained eigenvalue equation. In the following, we show the results for states with zero wave vectors parallel to the surface.

III. RESULTS AND DISCUSSIONS

A. Adiabatic potential energy surface

First of all, for our discussion, some high symmetry sites are introduced in Fig. 2, namely, the top site (TP), which is located directly above a surface Cu atom; the bridge site (BR), which is located above the midpoint between two surface Cu atoms; the hollow site (HL), which is located in the hollow surrounded by four surface Cu atoms; the long bridge site (LB), which is located above the midpoint between two adjacent surface Cu atoms lying along the [100] direction for Cu(110); the short bridge site (SB) which is located above the midpoint between two adjacent surface Cu atoms lying along the $[1\bar{1}0]$ direction for the Cu(110) surface; and the pseudothreefold site (PT), which is located at the midpoint of two first layer Cu atoms lying along the $[1\bar{1}0]$ direction and the nearest second layer Cu atom on the Cu(110) surface.

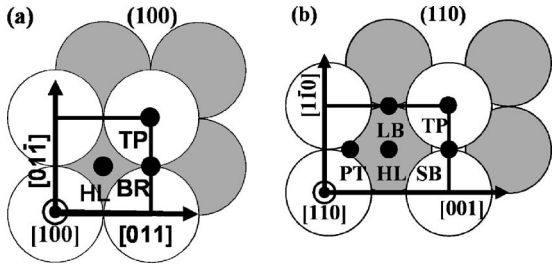

FIG. 2. Supercell geometries (only two layers shown) of (a) Cu(100) and (b) Cu(110) surfaces, with their high symmetry sites indicated by the small black circles: TP, top; BR, bridge; LB, long bridge; SB, short bridge; HL, hollow; and PT, pseudothreefold. The white and gray-colored circles correspond to the substrate atoms in the first and second layers, respectively. The origin of of the PES for hydrogen atom motion is taken as the position of the first layer atoms.

The potential energy surface at the equilibrium height of the hydrogen atom from the Cu(100) surface, has its lowest value −2.485 eV at the HL site, which is lower in energy by 168 meV as compared to that on the BR site. The potential energy on Cu(110), on the other hand, has its lowest value −2.353 eV at the SB site. The value at the SB site is higher by 22, 85 and 289 meV than at the PT site, the LB site, and the HL site, respectively. Figure 1 shows a diagonal view of the PES for the hydrogen atom on the Cu(100)[(110)] surface, the top view along the [100]([110]) axis and the side view along the $[01\bar{1}]$ ($[1\bar{1}0]$) axis, respectively, and shows energy isosurfaces that describe the PES in the range between −2.00 and −2.50 (−2.35) eV for the Cu(100)[(110)] surface. In increasing shading depth, the PES is represented by isosurfaces with values of −2.0, −2.20, −2.30, −2.40, −2.45, and −2.48 eV (−2.0, −2.10, −2.16, −2.26, −2.30, and −2.34 eV) in the case of the (100)[(110)] surface. The Cu atoms are located at (0.00,0.00,0.00), (2.55,0.00,0.00), (0.00,2.55,0.00), and (2.55,2.55,0.00) [(0.00,0.00,0.00), (3.64,0.00,0.00), (0.00,2.55,0.00), and (3.64,2.55,0.00)] on Cu(100)[(110)]. Here, the origin of the z coordinate is defined as the center of the 1st atom layer. A quick inspection of the obtained PESs shows that the PES on Cu(100) has only one large well centered on the HL site, and in contrast, the PES on Cu(110) has two rather isolated wells centered on the SB and LB sites. These results are in good agreement with calculations by Lai *et al.*,[8] Sundell *et al.*,[9] and Bae *et al.*[16]

B. Quantum states of a hydrogen atom on Cu(100)

Figures 3 and 4 display the diagonal view, the top view (along the [100] axis), and the side view (along the $[01\bar{1}]$ axis), of the wave functions for H atom motion on Cu(100).

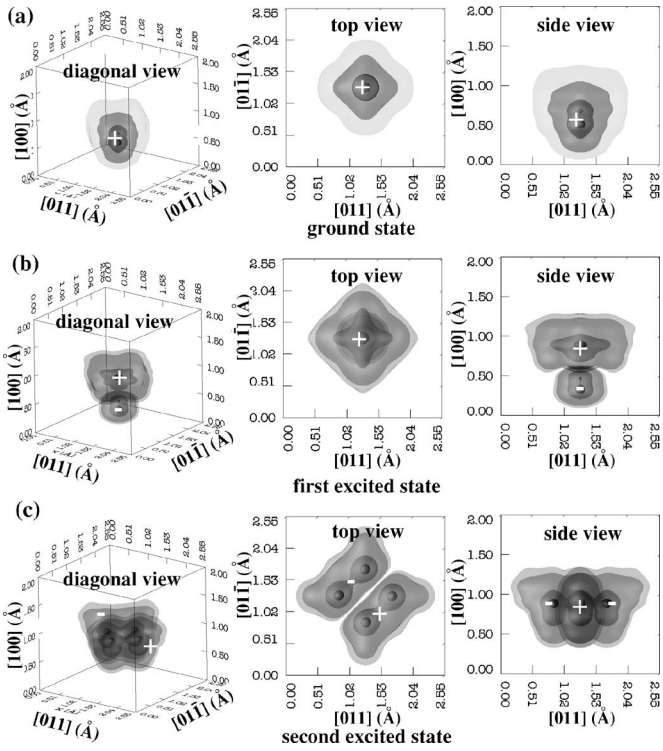

FIG. 3. Wave function at the (a) ground state, (b) first excited state, and (c) second excited state for H atom motion on Cu(100), taken from a diagonal view, top view (along the [100] axis) and side view of (along the $[01\bar{1}]$ axis). The labels "+" and "−" indicate the positive and negative valued regions of wave functions, respectively. The absolute value of the wave function increases with increasing isosurface shading depth.

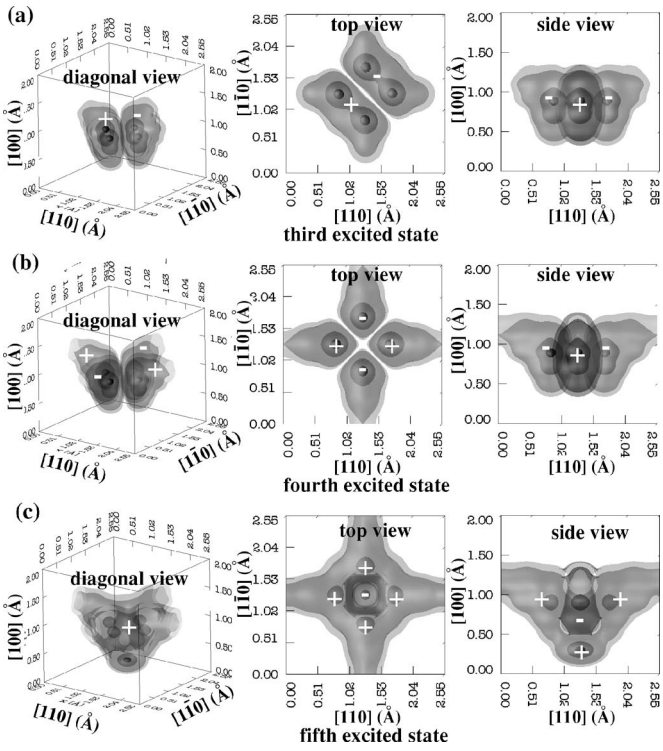

FIG. 4. (a) Same as Fig. 3(a), but for the third, (b) fourth, and (c) fifth excited states.

These results show that the ground state wave function for H atom motion on Cu(100) is strongly localized on the HL site, as shown in Fig. 3(a). Referring to Fig. 3(b), the first excited state wave function has a character that would best describe this state as a vibrational mode perpendicular to the surface. In Figs. 3(c) and 4(a), the second and third excited state wave functions have only one node and vibrational characters along the [001] and [010] directions, respectively. The fourth excited state wave function in Fig. 4 shows that there is one node in along each of the [010] and [001] directions. Thus, the wave functions at the second, third and fourth excited states show characters of vibrational modes in the direction parallel to the surface. In Fig. 4(c), the fifth excited state wave function can be seen as distributed from the HL site to the BR site with no nodes, that is to say, the delocalization of the wave function is continuous. The characters of the wave functions are summarized in Table III. It is finally noted that the wave functions for D and T atom motion on Cu(100) have the same features as the H atom.

C. Quantum states of a hydrogen atom on Cu(110)

Figures 5–7 displays the diagonal view, the top view (along the [110] axis) and the side view (along the $[1\bar{1}0]$ axis) of the ground and excited state wave functions for H atom motion on Cu(110). Figures 6(a) and 7(a) show the side

TABLE III. The number of nodes and vibrational character of the wave functions for H atom motion on Cu(100) and Cu(110).

Cu(100) excited state	[010]	[001]	[100]	vibrational mode
0	0	0	0	localized
1	0	0	1	perpendicular
2	0	1	0	parallel
3	1	0	0	parallel
4	1	1	0	parallel
5				

Cu(110) excited state	[001]	$[1\bar{1}0]$	[110]	vibrational mode
0	0	0	0	localized
1	1	0	0	parallel
2	2	0	0	parallel
3	3	0	0	parallel
4	0	0	0	localized
5	4	0	0	parallel
6	6	1	0	parallel
7	5	0	0	parallel
8	0	1	0	parallel
9	6	1	0	parallel
10	2	0	1	perpendicular

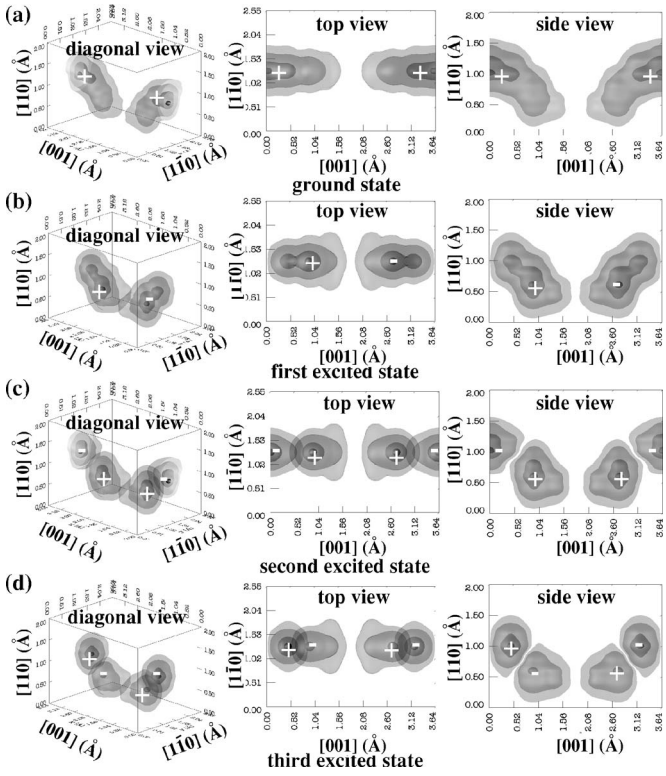

FIG. 5. Wave function at the (a) ground state, (b) first excited state, (c) second excited state, and (d) third excited state for H atom motion on Cu(110), taken from a diagonal view, top view, top view (along the [110] axis) and side view (along the [1$\bar{1}$0] axis), respectively. The labels "+" and "−" indicate the positive and negative valued regions of the wave functions, respectively. The absolute value of the wave function increases with increasing isosurface shading depth.

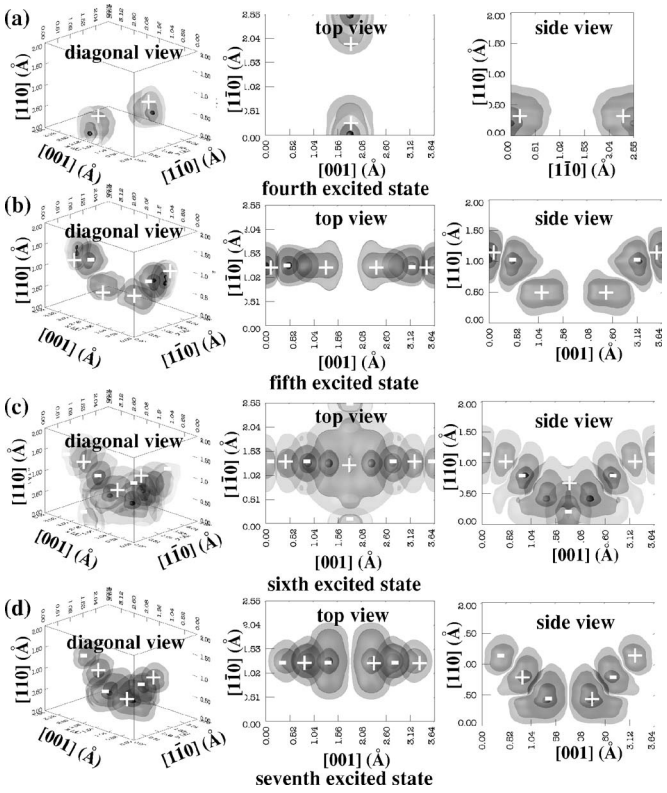

FIG. 6. (a) Same as Fig. 5(a), but for the fourth, taken from side view along the [001] axis, (b) fifth, (c) sixth, and (d) seventh excited states.

view along the [001] axis. The ground state wave function for H atom motion on Cu(110) is mainly localized in the region from the SB site to both of its two neighboring PT sites, as shown in Fig. 5(a). In Figs. 5 and 6, the wave functions at the first, second, third, fifth, and seventh excited states have one, two, three, four, and five nodes and vibrational characters centered at the SB site along the [001] direction. Moreover, the wave functions follow the structure of the PES around the SB site, as shown in the rightmost panels in Fig. 1(b). Thus, they show characteristics of vibrational modes along the [001] axis, centered at the SB site. The excitation to these states from the ground state correspond to vibrational excitations parallel to the surface. According to Fig. 6(a), the fourth excited state wave function is localized strongly on the LB site. Figure 7(a) shows that the wave function has one node along the [1$\bar{1}$0] direction, and that the excitation to the eighth excited state from the fourth excited state is a vibrational excitation parallel to the [1$\bar{1}$0] axis.

The more delocalized natures of the sixth and ninth excited state wave functions are exhibited in Figs. 6(c) and 7(b), as these wave functions are spread enough to access both the SB and LB sites. Moreover, these wave functions have six nodes and one node along the [001] and [1$\bar{1}$0] directions, respectively. Figure 7(c) shows that the wave function has two nodes and one node along the [001] and [110] directions, respectively. The excitation to the tenth excited state from the ground state on the other hand corresponds to a vibrational excitation perpendicular to the surface. The characters of the wave functions are summarized in Table III.

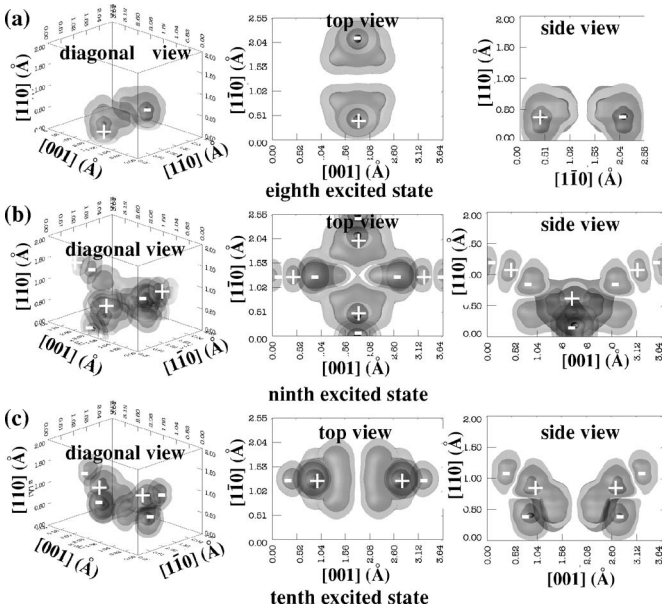

FIG. 7. (a) Same as Fig. 5(a), but for the eighth, taken from side view along the [001] axis, (b) ninth, and (c) tenth excited states.

D. Isotope effect

The wave functions of D and T atoms on Cu(110) have the same features with that for the H atom, although the ordering is slightly changed. More precisely, the fourth excited state wave function for H atom motion on Cu(110) is strongly localized on the LB site as shown in Fig. 6(a), while those for D and T atom motion show vibrational modes parallel to the surface. On the other hand, the fifth excited state wave functions for D and T atom motion on Cu(110) are localized on the LB site and that for the H atom motion shows a vibrational character parallel to the surface as shown in Fig. 6(b). Referring to the adiabatic PES for hydrogen atom motion on Cu(110) [Fig. 1(b)], the breadth of the PES around the SB site is not large as compared to that on the LB site. To Noting the small mass of the hydrogen atom, quantum effects should thus be prominent here.

The lighter mass of the H atom as compared with a D atom implies more widely spaced energy eigenvalues on a local potential well, i.e., a region classically set apart by a barrier, such as the potential minimum regions associated with the bridge sites, separately. From this it is thus not surprising that the H atom starts to access the LB site in a lower quantum number as compared with its heavier counterparts, explaining the apparent exchange of fourth and fifth eigenstates when comparing results of the different isotopes. Similar exchanges are also seen in higher excited states.

E. Discussions of characters of wave functions

The reason for the difference in the natures of the ground state wave function for hydrogen atom motion on the Cu(100) and Cu(110) faces is as follows. In the case of Cu(100), the depth of the three dimensional potential on the HL site is larger than on the other sites, as shown in Fig. 1(a). On the other hand, the PES on Cu(110) [Fig. 1(b)] shows the minimum potential energy at the SB site, and a small energy barrier between the SB site and the PT site. Thus the ground state wave function on Cu(100) is expected to strongly localize in the vicinity of the HL site only, and that on Cu(110) is expected to distribute from the SB site to both of its two neighboring PT sites.

The excited state wave functions on Cu(100) exhibit characters of vibrational modes centered at the HL site. The excited state wave functions on Cu(110) on the other hand show vibrational modes parallel to the surface centered not only at the SB site but also at the LB site, as shown in Figs. 6(a) and 7(a). These differences result from the differences in the PESs. For one, there's an obvious difference on symmetries: the Cu(110) unit cell has a twofold symmetry, while that for Cu(100) is fourfold. The PES on Cu(110) furthermore shows a large energy barrier centered at the HL site, thus defining two rather isolated wells centered at the SB and LB sites. It is from this that we obtain vibrational modes at the SB and LB sites separately within the lower excited states, i.e., the wave function does not spread from the SB site to the LB site.

On surface diffusion, the hydrogen atom on Cu(100) can hop into equivalent surface sites by tunneling, or directly over the energy barrier at the BR site when it is excited to an energy level that exceeds the activation energy obtainable from the PES. The fifth excited state wave function [Fig. 4(c)], especially when compared with the very much localized character of the ground state [Fig. 3(a)], shows delocalization that implies a clear capacity for adsorbate diffusion to proceed. This character of the diffusion on Cu(100) was pointed out in Refs. 9 and 14. In the case of Cu(110), the ground state and the lower excited states wave functions do not show delocalized characters that spread over both types of bridge sites until higher states [e.g. sixth, ninth excited states, as shown in Figs. 6(c) and 7(b)]. These results suggest the hydrogen atom cannot diffuse from the SB site to the LB site by tunneling, i.e., it diffuses over the energy barrier along the path connecting the adjacent SB and the LB sites.

TABLE IV. Experimental and calculated results of vibrational energies for H and D atom motion on Cu(100) and Cu(110).

	Cu(100)		Cu(110)	
	H	D	H	D
This work	90.8	67.2	144	116
W. Lai *et al.* (Ref. 8)	71.2	51.5		
P. G. Sundell *et al.* (Ref. 9)	71	50		
J. Kua *et al.* (Ref. 15)	92	67		
Chorkendorff *et al.* (Ref. 10)	69.5	52		
Lauhon *et al.* (Ref. 12)	70	51		
Astaldi *et al.* (Ref. 11)			118	80

Our calculation results for the quantum states of the hydrogen atom adsorbed on the Cu(100) and the Cu(110) surfaces are compared with previous experimental and theoretical studies and summarized in Table IV. In the STM-IETS experiments, a tunneling current I is measured as a function of bias voltage V across the junction and the vibrational energy of the adsorbed atom on the surface is derived from a peak of the d^2I/dV^2 curve as a function of the sample bias voltage.[28] In HREELS experiments, a scattering electron interacts only with the surface-perpendicular component of the dipole moment of the adsorbed atom,[2] and the scattering electron's loss energy corresponds to the vibrational excitation energy. In our results, the first excited state wave function for the H and D atom motion on Cu(100) corresponds to a vibrational mode perpendicular to the Cu(100) surface as shown in Fig. 3(b). The first excited state of the H (D) atom is 90.8 meV (67.2 meV) from the ground state, as shown in Table III. These values are in fair agreement with previous calculations[8,9,15] and the HREELS spectrum peaks at 69.5 and 52.0 meV observed by Chorkendorff *et al.*,[10] which correspond to H and D atom vibrational modes perpendicular to the Cu(100) surface. Lauhon *et al.*[12] also investigated vibrational spectra of H and D atoms in the direction perpendicular to Cu(100) by STM-IETS and reported results of 70 meV (H) and 51 meV (D).

We take notice of the tenth excited state for the H (D) atom on Cu(110), which is a vibrational mode perpendicular to the surface, as shown in Fig. 7(c). The tenth excited state energy of the H (D) atom is 144 meV (116 meV) above the

ground state, which can be compared with the experiment carried out by Astaldi *et al.*[11] They observed an HREELS spectrum peak corresponding to a vibrational mode perpendicular to the Cu(110) surface at 118 meV (80 meV), in a coverage of 0.25 ML. In our calculation of the quantum states, the Morse potential is adopted for the interpolation of the PESs in order to complete calculations within a reasonable amount of time. The surface-normal breadth of the PESs may apparently be overestimated as compared with the real values, and the kinetic energy of the hydrogen atom is overestimated due to the quantum effects. Thus, our reported values are higher than other available results.

IV. SUMMARY

We calculated the wave functions and the eigenenergies for hydrogen (H, D, and T) atom motion on Cu(100) and Cu(110) as part of our investigations on the quantum mechanical behavior of adsorbed hydrogen (H, D, and T) atoms. In the case of Cu(100), the ground state wave function is localized on the HL site and the excited state wave functions show vibrational characters centered at the HL site. In the case of Cu(110), the ground state wave function for hydrogen atom motion is distributed from SB to PT sites. The excited state wave functions on Cu(110) show vibrational modes centered both at the SB site and at the LB site, and the hydrogen atom migrates from the SB site to the LB site over the energy barrier directly. These features are attributed to the structure of the calculated adiabatic PES for hydrogen atom motion. The depth of the three-dimensional potential on the HL site is larger than over other sites on the Cu(100) surface. The PES on Cu(110) shows a small energy barrier between the SB site and the PT site, and a large energy barrier between the SB site and the LB site. Moreover, the fourth excited state wave function for the H atom motion on Cu(110) shows a localized mode on the LB site, similar to the fifth excited state wave functions for D and T atom motion. We finally find that the vibrational energies of hydrogen atom motion on Cu(100) and (110) are fairly in agreement with available experimental findings. This study will be useful in understanding the quantum mechanical behavior of hydrogen on Cu surfaces.

ACKNOWLEDGMENTS

This work was partly supported by the Ministry of Education, Culture, Sports, Science, and Technology of Japan (MEXT), through their Special Coordination Funds for the 21st Century Center of Excellence (COE) program (G18) "Core Research and Advance Education Center for Materials Science and Nano-Engineering," and through their Grants-in-Aid for Scientific Research on Priority Areas (Developing Next Generation Quantum Simulators and Quantum-Based Design Techniques) and by the New Energy and Industrial Technology Development Organization (NEDO), through their program on "Research and Development of Polymer Electrolyte Fuel Cell Systems." Some of the calculations presented here were performed using the computer facilities of Cyber Media Center (Osaka University), the Institute of Solid State Physics (ISSP) Super Computer Center (University of Tokyo), the Yukawa Institute (Kyoto University), and the Japan Atomic Energy Research Institute (ITBL, JAERI).

*Electronic address: kasai@dyn.ap.eng.osaka-u.ac.jp

[1] K. Christmann, Surf. Sci. Rep. **9**, 1 (1988).
[2] M. J. Puska and R. M. Nieminen, Surf. Sci. **157**, 413 (1985).
[3] Y. Miura, W. A. Diño, H. Kasai, and A. Okiji, Surf. Sci. **507-510**, 838 (2002).
[4] W. A. Diño, Y. Miura, H. Nakanishi, H. Kasai, T. Sugimoto, and T. Kondo, Solid State Commun. **132**, 713 (2004).
[5] T. R. Mattsson, G. Wahnström, and L. Bengtsson, Phys. Rev. B **56**, 2258 (1997).
[6] S. C. Bãdescu, K. Jacobi, Y. Wang, K. Bedurftig, G. Ertl, P. Salo, T. Ala-Nissila, and S. C. Ying, Phys. Rev. B **68**, 205401 (2003).
[7] K. Nobuhara, H. Kasai, H. Nakanishi, and A. Okiji, J. Appl. Phys. **96**, 5020 (2004).
[8] W. Lai, D. Xie, J. Yang, and D. H. Zhang, J. Chem. Phys. **121**, 7434 (2004).
[9] P. G. Sundell and G. Wahnström, Phys. Rev. Lett. **92**, 155901 (2004).
[10] I. Chorkendorff and P. B. Rasmussen, Surf. Sci. **248**, 35 (1991).
[11] C. Astaldi, A. Bianco, S. Modesti, and E. Tosatti, Phys. Rev. Lett. **68**, 90 (1992).
[12] G. Lee and E. W. Plummer, Surf. Sci. **498**, 229 (2002).
[13] M. Rohwerder and C. Benndorf, Surf. Sci. **307-309**, 789 (1994).
[14] L. J. Lauhon and W. Ho, Phys. Rev. Lett. **85**, 4566 (2000).
[15] J. Kua, L. J. Lauhon, W. Ho, and W. A. Goddard III, J. Chem. Phys. **115**, 5620 (2001).
[16] C. Bae, D. L. Freeman, J. D. Doll, G. Kresse, and J. Hanfer, J. Chem. Phys. **113**, 6926 (2000).
[17] B. Hammer, M. Scheffler, K. W. Jacobsen, and J. K. Nørskov, Phys. Rev. Lett. **73**, 1400 (1994).
[18] P. Kratzer, B. Hammer, and J. K. Nørskov, Surf. Sci. **359**, 45 (1996).
[19] W. Brenig, S. Kuchenhoff, and H. Kasai, Appl. Phys. A: Solids Surf. **51**, 115 (1990).
[20] H. Kasai and A. Okiji, Surf. Sci. **283**, 233 (1993).
[21] W. A. Diño, H. Kasai, and A. Okiji, Prog. Surf. Sci. **63**, 63 (2000).
[22] N. B. Arboleda, Jr., H. Kasai, K. Nobuhara, W. A. Dino, and H. Nakanishi, J. Phys. Soc. Jpn. **73**, 745 (2004).
[23] S. J. Gulding, A. M. Wodtke, H. Hou, C. T. Rettner, H. A. Michelsen, and D. J. Auerbach, J. Chem. Phys. **105**, 9702 (1996).
[24] N. Ozawa, T. A. Roman, N. Nakanishi, and H. Kasai, Surf. Sci. **600**, 3550 (2006).
[25] See http://www.fysik.dtu.dk/
[26] J. P. Perdew, J. A. Chevary, S. H. Vasko, K. A. Jackson, M. R. Pederson, D. J. Singh, and C. Fiolhais, Phys. Rev. B **46**, 6671 (1992).
[27] W. G. Wyckoff, *Crystal Structures*, 2nd ed. (Krieger, New York, 1981).
[28] B. C. Stipe, M. A. Rezaei, and W. Ho, Science **280**, 1732 (1998).